An immersed boundary method based on the L^2-projection approach

M.G.C. Nestola, B. Becsek, H. Zolfaghari, P. Zulian, D. Obrist and R. Krause

Abstract In this paper we present a framework for Fluid-Structure Interaction simulations. Taking inspiration from the Immersed Boundary technique introduced by Peskin [1] we employ the finite element method for discretizing the equations of the solid structure and the finite difference method for discretizing the fluid flow. The two discretizations are coupled by using a volume based L^2–projection approach to transfer elastic forces and velocities between the fluid and the solid domain. We present results for a Fluid–Structure Intercation benchmark which describes self-induced oscillating deformations of an elastic beam in a flow channel.

Dr. Maria Giuseppina Chiara Nestola
Institute of Computational Science, Center for Computational Medicine in Cardiology (CCMC), Università della Svizzera italiana,Via Giuseppe Buffi 13, 9600 Lugano, Switzerland e-mail: nestom@usi.ch

Barna Becsek
ARTORG Center for Biomedical Engineering Research, University of Bern, Murtenstrasse 50 3008 Bern, Switzerland e-mail: barna.becsek@artorg.unibe.ch

Hadi Zolfaghari
ARTORG Center for Biomedical Engineering Research, University of Bern, Murtenstrasse 50 3008 Bern, Switzerland e-mail: hadi.zolfaghari@artorg.unibe.ch

Prof. Dr. Dominik Obrist
ARTORG Center for Biomedical Engineering Research, University of Bern, Murtenstrasse 50 3008 Bern, Switzerland e-mail: dominik.obrist@artorg.unibe.ch

Dr. Patrick Zulian
Institute of Computational Science, CCMC, Università della Svizzera italiana, Via Giuseppe Buffi 13, 9600 Lugano, Switzerland e-mail: patrick.zulian@usi.ch

Prof. Dr. Rolf Krause
Institute of Computational Science, CCMC, Università della Svizzera italiana, Via Giuseppe Buffi 13, 9600 Lugano, Switzerland e-mail: rolf.krause@usi.ch

1 Introduction

During the last decades, Fluid–Structure Interaction (FSI) [1, 2] has received considerable attention due to various applications where a fluid and a solid interact with each other (such as in aeronautics, turbomachinery, and biomedical applications).

Several approaches have been developed in order to reproduce the interaction between a fluid and a surrounding solid structure, which can be classified in boundary-fitted and embedded boundary methods. In the boundary-fitted methods, the fluid problem is resolved in a moving spatial domain over which the incompressible Navier-Stokes equations are formulated in an Arbitrary Lagrange Eulerian (ALE) framework [3] while the solid structure is usually described in a Lagrangian fashion. Although this approach is known to allow for accurate results at the interface between solid and fluid, for scenarios that involve large displacements and/or rotations, the fluid grid may become severely distorted, thus affecting both the numerical stability of the problem and the accuracy of the solution.

In order to circumvent those difficulties, embedded boundary approaches such as the Immersed Boundary Method (IBM), have been introduced to model the fluid-structure interaction on a stationary fluid grid analyzed in a Eulerian fashion. The main aspect of this technique is the representation of the immersed solid material as a force density in the Navier-Stokes equations.

In the IBM, the volume of the solid is commonly described by systems of fibres that resist extension, compression, or bending [1, 2, 4]. Some alternative approaches have been proposed on the basis of the finite element method for the spatial approximation of the Lagrangian quantities (force densities, displacement field, etc.). In all these approaches the reaction force exerted by the solid on the fluid is computed *explicitly* by using the fluid velocity field to get the corresponding displacement of the solid structure [5, 6, 7].

We describe an alternative framework for FSI simulations, where we employ the finite difference method for simulating the fluid flow and couple it with a finite element method for the structural problem. The main novelties of this work are (I) the description of the solid body motion obtained by solving *implicitly* the elastodynamic equations and (II) the treatment of the Lagrangian-Eulerian interaction which is achieved by means of the L^2– projection. Such approach allows for the transfer of data between non-matching structured (Cartesian) and unstructured meshes arbitrarily distributed among different processors.

All the modules of the FSI computational frameworks are integrated into the multi-physics simulation framework MOOSE (`mooseframework.org`). The code is optimised for modern hybrid high-performance computing platforms such as the Cray XC50 system at the Swiss National Supercomputing Centre CSCS.

2 Strong Formulation of the FSI Problem

In this section we provide a brief description of the methodology adopted in our framework to solve the FSI problem. Since the proposed approach follows the main

principle of the IBM, we employ the standard Eulerian formulation for the Navier-Stokes equations for incompressible flows, whereas the elastic response of the embedded structure is described in a Lagrangian fashion.

Let $\Omega \subset \mathbb{R}^d$ (with $d = 1,2,3$) be a bounded Lipschitz domain denoting the physical region occupied by the coupled fluid-structure system. We label $\mathbf{x} \in \Omega$ as the spatial point, and $\widehat{\mathbf{x}} \in \widehat{\Omega}_s$ as the material (or reference) point, with $\widehat{\Omega}_s \subset \mathbb{R}^d$ denoting the material (reference) configuration of the solid domain (Fig. 1).

We assume that the map $\widehat{\boldsymbol{\chi}} : \widehat{\Omega}_s \times I \to \mathbb{R}^d$ is a one-to-one correspondence between the material $\widehat{\mathbf{x}}$ and the actual $\mathbf{x}$ positions occupied by the elastic structure during the time interval $I = [0\ \mathrm{T}]$, s. t. $(\widehat{\mathbf{x}}, t) \to \mathbf{x} = \widehat{\boldsymbol{\chi}}(\widehat{\mathbf{x}}, t), \forall t \in I$. Additionally, we denote with Γ_{fsi} the physical interface between the fluid and the solid mesh.

The strong formulation of the complete FSI problem reads as follows:

$$
\begin{aligned}
\widehat{\rho}_{s0} \frac{\partial^2 \widehat{\mathbf{u}}_s}{\partial t^2} - \widehat{\nabla}_{\widehat{\mathbf{x}}} \cdot \widehat{\mathbf{P}} &= \mathbf{d} && \text{on} \quad \widehat{\Omega}_s \quad (a) \\
\rho_f \frac{\partial \mathbf{v}_f}{\partial t} + \rho_f \left(\mathbf{v}_f \cdot \nabla\right) \mathbf{v}_f + \nabla p_f - \mu \Delta \mathbf{v}_f &= \mathbf{f}_{\mathrm{fsi}} && \text{on} \quad \Omega \quad (b) \\
\nabla \cdot \mathbf{v}_f &= 0 && \text{on} \quad \Omega \quad (c) \\
\mathbf{v}_f &= \frac{\partial \mathbf{u}_s}{\partial t} && \text{on} \quad \Gamma_{\mathrm{fsi}} \quad (d)
\end{aligned}
\tag{1}
$$

Here Eq. 1(a) is the equation of the elastodynamics where $\widehat{\rho}_{s0}$ is the mass density per unit undeformed volume of the elastic structure, $\widehat{\mathbf{u}}_s = \widehat{\mathbf{u}}_s(\widehat{\mathbf{x}}, t)$ is the related displacement field, $\widehat{\mathbf{P}} = \widehat{\mathbf{P}}(\widehat{\mathbf{x}}, t)$ is the first Piola-Kirchhoff stress tensor, $\mathbf{d}$ is a prescribed external body force, and $\widehat{\nabla}_{\widehat{\mathbf{x}}} \cdot$ is the divergence operator computed in the reference configuration. For an hyperelastic material, the first Piola-Kirchhoff stress tensor $\widehat{\mathbf{P}}$ is related to the deformation through a constitutive equation derived from a given scalar valued energy function Ψ, i. e. $\widehat{\mathbf{P}} = \widehat{\mathbf{F}} \frac{\partial \psi(\widehat{\mathbf{E}})}{\partial \widehat{\mathbf{E}}}$, where $\widehat{\mathbf{E}} := 1/2(\widehat{\mathbf{F}}^T \widehat{\mathbf{F}} - \mathbf{I})$ is the Lagrangian-Green strain tensor and $\widehat{\mathbf{F}}$ is the deformation gradient tensor defined as $\widehat{\mathbf{F}} = \nabla_{\widehat{\mathbf{x}}} \mathbf{x}$.

Eq.s 1(b-c) represent the standard Navier-Stokes equations where ρ_f is the fluid density, $\mathbf{v}_f$ is the velocity field of the fluid, p_f is the pressure, $\nabla_{\mathbf{x}}$ is the gradient operator, $\Delta_{\mathbf{x}}$ is the Laplacian operator computed in the current configuration and $\mathbf{f}_{\mathrm{fsi}}$

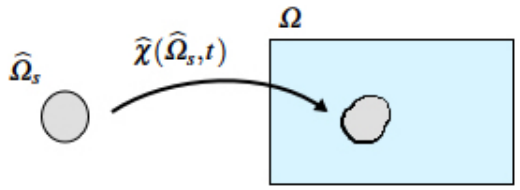

Fig. 1 Lagrangian (left) and Eulerian (right) coordinate systems adopted in the Immersed Boundary method.

is the force density generated by the embedded solid structure as we will describe in Section 3.1.

Remark In the equation of the elastodynamics, i. e. Eq. 1(a), the evaluation of the inertial term must take care of the fluid in which it is embedded. This can be done by subtracting the density of the fluid phase from the solid one (i.e. $\widehat{\rho}_{s0} - \rho_f$) [14]. It is worth to pointing out that, since in our case the fluid velocity field is used to recover the displacement of the FSI interface, this difference is restricted only to Γ_{fsi}.

3 Discretization of the FSI problem

In this section, we provide some details about the discretization in time and in space of the solid and the fluid sub-problem.

3.1 Solid Problem

For the time discretization of the solid problem, we adopt the classical Newmark scheme. This scheme is based on a Taylor expansion of the displacements and the velocities:

$$\widehat{\mathbf{u}}_{s,n+1} = \widehat{\mathbf{u}}_{s,n} + \Delta t\ \mathbf{v}_{s,n} + \tfrac{\Delta t^2}{2}((1-2\beta)\mathbf{a}_{s,n} + 2\beta\mathbf{a}_{s,n+1})$$

$$\widehat{\mathbf{v}}_{s,n+1} = \widehat{\mathbf{v}}_{s,n} + \Delta t\ ((1-\alpha)\widehat{\mathbf{u}}_{s,n} + \alpha\widehat{\mathbf{a}}_{s,n+1})$$

where Δt is the time step size, $\mathbf{a}_s := \frac{\partial^2 \widehat{\mathbf{u}}_s}{\partial t^2}$ and $\mathbf{v}_s := \frac{\partial \widehat{\mathbf{u}}_s}{\partial t}$ are the the acceleration and the velocity of the solid, respectively, and the parameters α and 2β are chosen such that $\alpha = 2\beta = 1/2$.

For the spatial discretization of the structure problem, we assume that the solid domain $\widehat{\Omega}_s$ can be approximated by a discrete domain $\widehat{\Omega}_s^h$ and the associated mesh $\widehat{T}_s^h = \{\widehat{E}_s \subseteq \widehat{\Omega}_s^h | \bigcup \widehat{E}_s = \widehat{\Omega}_s^h\}$, where its elements $\widehat{E}_s$ form a partition. The Galerkin formulation of the elastodynamics equation reads:

For every $t \in (0;T]$ find $\widehat{\mathbf{u}}_s^h(\cdot,t) \in \widehat{\mathbf{V}}_s^h := [\widehat{V}_s^h(\widehat{T}_s^h)]^d \subset [H_0^1(\widehat{\Omega}_s)]^d$ so that:

$$(\widehat{\rho}_{s0}\widehat{\mathbf{a}}_s^h, \delta\mathbf{u}_s^h) + a(\mathbf{u}_s^h, \delta\mathbf{u}_s^h) - (\mathbf{d}_s^h, \delta\mathbf{u}_s^h) = \mathbf{0} \tag{2}$$

By defining $(\mathbf{F}^h, \delta\mathbf{u}_s^h) = a(\mathbf{u}_s^h, \delta\mathbf{u}_s^h) - (\mathbf{d}_s^h, \delta\mathbf{u}_s^h)$ and using the Green's formula we get:

$$(\widehat{\rho}_{s0}\widehat{\mathbf{a}}_s^h, \delta\mathbf{u}_s^h) + (\mathbf{F}^h, \delta\mathbf{u}_s^h) = (\mathbf{f}_{\text{fsi}}^h, \delta\mathbf{u}_s^h)_{L^2(\Gamma_{\text{fsi}}^h)} \tag{3}$$

where $\mathbf{f}_{\text{fsi}}^h$ represents the reaction force exerted by the solid structure on the fluid.

3.2 Fluid Problem

The time integration of the fluid problem is carried out by a 3rd order low-storage Runge-Kutta scheme for both the advective and the diffusion terms [8].

For the discretization of Eq. 1(b), the usage of high-order (sixth) explicit-finite differences leads to a linear system of equations of the form:

$$\begin{bmatrix} \mathbf{H} & \mathbf{G} \\ \mathbf{D} & \mathbf{0} \end{bmatrix} \begin{bmatrix} \mathbf{v}_f \\ \mathbf{p}_f \end{bmatrix} = \begin{bmatrix} \mathbf{z} \\ \mathbf{0} \end{bmatrix}$$

Here the matrices $\mathbf{D}$ and $\mathbf{G}$ are the spatial discretization of the divergence and the gradient operators, $\mathbf{z}$ is the discrete representation of the right hand side, whereas $\mathbf{H}$ is the Helmholtz operator which coincides with the identity matrix (except for the boundary conditions) due to the usage of a purely explicit time integration scheme. By applying $\mathbf{D}$ to the equation $\mathbf{H}\mathbf{v}_f + \mathbf{G}\mathbf{p}_f = \mathbf{0}$, one may derive the following equation for the pressure:

$$\mathbf{D}\mathbf{H}^{-1}\mathbf{G}\mathbf{p}_f = \mathbf{D}\mathbf{H}^{-1}\mathbf{z} \tag{4}$$

In order to guarantee the gradient of the pressure to be unique, the Schur complement $\mathbf{D}\mathbf{H}^{-1}\mathbf{G}$ must be h-elliptic (i.e. must have only one zero eigenvalue). To this aim Arakawa-C grids are adopted which combine several types of nodal points located in different geometrical positions.

4 L^2 - projection

For coupling the two sub-problems we adopt a volume L^2–projection which allows for the transfer of discrete fields between non conforming meshes arbitrarily distributed among several processors. Such an approach ensures convergence, efficiency, flexibility and accuracy without requiring a priori information on the relation between the different meshes. To this aim, we attach Lagrangian basis functions to the finite difference discretization [9], define the corresponding finite element space as $\mathbf{V}_f^h = \mathbf{V}_f^h(T_f^h) \subset [H_0^1(\Omega)]^d$ and introduce the vector of Lagrange multipliers $\boldsymbol{\lambda}_{\text{fsi}}^h$ with the related virtual variations, $\delta\boldsymbol{\lambda}_{\text{fsi}}^h \in \mathbf{M}_{\text{fsi}}^h(\widehat{T}_s^h \cap T_f^h) \subset [H^1(\widehat{\Omega}_s \cap \Omega)]^d$, where T_f^h represents the fluid grid.

In the following, the projection operator $\mathbb{P} : V_f^h \to V_s^h$ is defined by focusing on the scalar case, which means that for each component of the velocity $v_{f,i}^h \in V_f^h$, we may find $w_{s,i}^h = \mathbb{P}(v_{f,i}^h) \in \widehat{V}_s^h$, such that the following weak-equality condition holds:

$$\int_{\widehat{T}_s^h \cap T_f^h} (v_{f,i}^h - \mathbb{P}(v_{f,i}^h))\delta\lambda_{fsi}^h \, dV = \int_{\widehat{T}_s^h \cap T_f^h} (v_{f,i}^h - w_{s,i}^h)\delta\lambda_{\text{fsi}}^h \, dV = 0 \qquad \forall\ \delta\lambda_{\text{fsi}}^h \in M_{\text{fsi}}^h \tag{5}$$

By writing v_f^h, w_s^h and $\delta\lambda_{\text{fsi}}^h$ in term of basis functions (here the index i is omitted for a simpler notation), i.e. $v_f^h = \sum_{l \in J_f} v_f^l N_f^l$, $w_s^h = \sum_{j \in J_s} w_s^j N_s^j$ and $\delta\lambda_{\text{fsi}}^h = \sum_{k \in J_{\text{fsi}}} \delta\lambda_{\text{fsi}}^k N_{\text{fsi}}^k$ (where J_s, J_f and J_{fsi} are index sets), we get the so called mortar integrals: $B_{k,l} = \int_{I_h} N_f^l N_{\text{fsi}}^k \, dV$ and $S_{k,j} = \int_{I_h} N_s^j N_{\text{fsi}}^k \, dV$. Equation 5 can be then written in the following algebraic form:

$$\mathbf{w}_s = \mathbf{S}^{-1}\mathbf{B}\mathbf{v}_f = \mathbf{T}\mathbf{v}_f \tag{6}$$

The transpose of $\mathbf{T}$ is used to transfer the reaction force from the solid to the fluid grid.

In order to reduce the computational cost required to compute the inverse of the matrix $\mathbf{S}$, we adopt dual basis functions for the function space $\mathbf{M}^h_{\text{fsi}}$. In this case this function space is spanned by a set of functions which are biorthogonal to the basis functions of $\widehat{\mathbf{V}}^h_s$ with respect to the L^2-inner product:

$$(N^k_{\text{fsi}}, N^j_s)_{L^2(I_h)} = \delta^{k,j}(N^j_s, \mathbf{1})_{L^2(I_h)} \quad \forall k, j \tag{7}$$

The usage of the dual basis functions corresponds to replacing the standard L^2–projection with a Pseudo–L^2–projection, which allows for a more efficient evaluation of the transfer operator $\mathbf{T}$ since the matrix $\mathbf{S}$ becomes diagonal. The assembly of the transfer operator is done in several steps [10]: (a) we compute the overlapping region by means of a tree search algorithm, (b) generate the quadrature points for integrating in the intersecting region, (c) compute the local element-wise contributions for the operators $\mathbf{B}$ and $\mathbf{S}$ by means of numerical quadrature, and (d) assemble the two mortar matrices.

5 Overview of the FSI algorithm

In our framework a segregated approach is adopted to solve the fully coupled FSI problem. More specifically, we use a fixed point (Picard) iteration scheme for solving the arising coupled non-linear discrete system.

For a given time step n and given a starting solution at the Picard iteration l, the following steps are performed within iteration $l+1$:

Step 1: Velocity values are transferred from the fluid grid to the solid mesh.
Step 2: The elastodynamic equation (Eq. 1(a)) is solved with the Dirichlet boundary conditions (Eq. 1(d)).
Step 3: The reaction force $\mathbf{f}_{\text{fsi}}$ is computed and transferred from the solid mesh to the fluid grid.
Step 4: The Navier-Stokes problem (Eq. 1(b)-(c)) is solved by using the force $\mathbf{f}_{\text{fsi}}$ as source term.
Step 5: Suitable residual norms are computed between the FSI interaction force terms evaluated at iterations l and $l+1$, i. e. $\|\mathbf{f}^{l+1}_{\text{fsi}} - \mathbf{f}^{l}_{\text{fsi}}\|_\infty / \|\mathbf{f}^{0}_{\text{fsi}}\|$ for the relative convergence criterion and $\|\mathbf{f}^{l+1}_{\text{fsi}} - \mathbf{f}^{l}_{\text{fsi}}\|_\infty$ for the absolute convergence criterion [6], and compared with given threshold values. This ensures the satisfaction of the coupling between the two sub-problems, thus leading to either a new Picard iteration or a new time step $n+1$ otherwise.

We employ the numerical solver IMPACT (**I**ncompressible (Turbulent) flows on **M**assively **PA**rallel **C**ompu**T**ers) for solving the non-dimensional Navier-Stokes equations [8]. The solid problem and the assembly of the transfer operator are implemented in the finite-element framework MOOSE (`www.mooseframework.org`), whereas the library MOONoLiTH (`https://bitbucket.org/zulianp/par_moonolith`) is used for detecting the overlapping region between the fluid and the solid grids and computing the corresponding intesections.

6 Numerical Results

In this section we present results related to the Turek-Hron FSI benchmark which considers the incompressible flow of a Newtonian fluid around an elastic solid structure composed of a disk and a rectangular trailing beam.

The dimensions of the fluid channel are (Fig. 2 (a)): length $L_f = 3.0\,m$ and height $H_f = 0.41\,m$. The disk center is positioned at $C = (0.2\,m, 0.2\,m)$ (measured from the left bottom corner of the channel) and the radius is $r = 0.05\,m$. The elastic structure bar has length $L_s = 0.35\,m$ and height $H_s = 0.02\,m$; the right bottom corner is positioned at $(0.6\,m, 0.19\,m)$, and the left end is fully attached to the circle. The fluid properties are $\rho_f = 1000\,kg/m^3$ and $\mu = 1\,Pa \cdot s$ which lead to a Reynolds number of 200. The density of the solid structure is the same as the fluid phase, and a Saint-Venant Kirchhoff model is adopted as constitutive law, for which the first Piola-Kirchhoff stress tensor is defined as: $\widehat{\mathbf{P}} = \widehat{\mathbf{F}}(\lambda\ \mathrm{tr}(\widehat{\mathbf{E}})\mathbf{I} + 2\mu\widehat{\mathbf{E}})$ with $\mu = 2.0\,MPa$ and $\lambda = 4.7\,MPa$. Periodic boundary conditions are imposed along the inlet and the outlet of the fluid channel together with no-slip boundary conditions on the top and the bottom. Moreover at the inlet a Poiseuille flow with a centerline velocity of $1.5\,m/s$ is enforced by a fringe region appended downstream.

In Fig. 2 (b) we show the displacements in x and y direction of a control point P located at the end of the elastic beam ($A \equiv (0.6\,m,\ 0.2\,m)$, Fig. 2 (a)). The amplitude of the last period of oscillation is in the range of $0.03\,m$ for the vertical displacement and of $0.0025\,m$ for the horizontal displacement; the frequency of the y-displacement is about $6\,s^{-1}$, and the frequency for the x-displacement is about $11\,s^{-1}$. All values are in good agreement with the original benchmark results [11]. In Fig. 2 (c) we also show the forces exerted by the lift and drag forces acting on the cylinder and the beam structure together. Again the values agree well with the results obtained by other numerical methods applied to the same problem [12]. Finally, the fluid

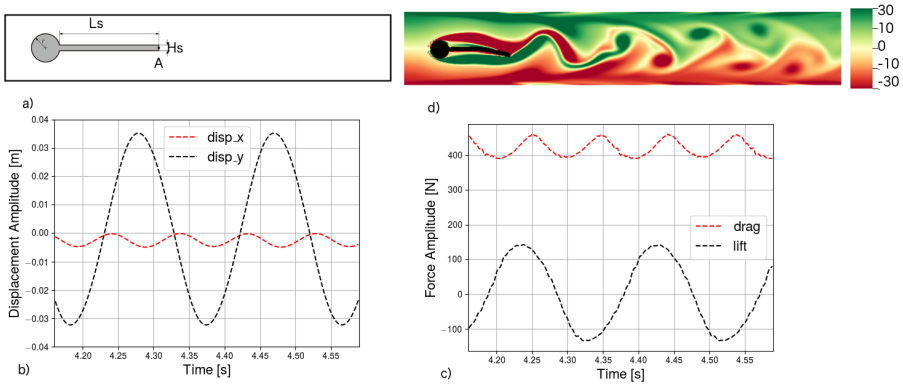

Fig. 2 (a) Geometry of the Turek-Hron benchmark. (b) Amplitude displacement in x and y direction of a control point A located at the end of the elastic beam. (c) Lift and drag forces. (d) Fluid vorticity.

vorticity is depicted in Fig. 2 (d) ranging from $-30\,s^{-1}$ to $30\,s^{-1}$, in agreement with numerical values reported in Griffith [13] .

7 Conclusion

In this article we present a novel FSI framework based on the IMB. The description of the solid motion, obtained by solving *implicitly* the elastodynamic equations, ensures to yield extra stability and robustness. Moreover, the use of the fluid solver IMPACT and of the software MOONoLith for the L^2-projection allows for a completely parallel framework suitable for the simulation of complex and large simulations such the blood flow in human arteries and through heart valves.

References

1. Peskin, Charles S."Flow patterns around heart valves: a numerical method." Journal of computational physics 10.2 (1972): 252-271.
2. Liu, Wing Kam, et al."Immersed finite element method and its applications to biological systems." Computer methods in applied mechanics and engineering 195.13 (2006): 1722-1749.
3. Nestola, Maria GC, et al. "Three-band decomposition analysis in multiscale FSI models of abdominal aortic aneurysms." International Journal of Modern Physics C 27.02 (2016): 1650017.
4. Devendran, Dharshi, and Charles S. Peskin."An immersed boundary energy-based method for incompressible viscoelasticity." Journal of Computational Physics 231.14 (2012): 4613-4642.
5. Griffith, B. E., and Luo, X. (2017). "Hybrid finite difference/finite element immersed boundary method". International journal for numerical methods in biomedical engineering. 33.12 (2017).
6. Gil, Antonio J., et al. The immersed structural potential method for haemodynamic applications. Journal of Computational Physics 229.22 (2010): 8613-8641.
7. Boffi, D., et al. On the hyper-elastic formulation of the immersed boundary method. Computer Methods in Applied Mechanics and Engineering 197.25 (2008): 2210-2231.
8. Henniger, Rolf, Dominik Obrist, and Leonhard Kleiser."High-order accurate iterative solution of the Navier-Stokes equations for incompressible flows." PAMM 7.1 (2007): 4100009-4100010.
9. Fackeldey, K., et al. "Coupling molecular dynamics and continua with weak constraints". Multiscale Modeling and Simulation, 9.4 (2011) 1459-1494.
10. Krause, Rolf, and Patrick Zulian."A parallel approach to the variational transfer of discrete fields between arbitrarily distributed unstructured finite element meshes." SIAM Journal on Scientific Computing 38.3 (2016): C307-C333.
11. Turek, Stefan, and Jaroslav Hron."Proposal for numerical benchmarking of fluid-structure interaction between an elastic object and laminar incompressible flow." Springer Berlin Heidelberg, 2006. 371-385.
12. Turek, Stefan, et al."Numerical benchmarking of fluid-structure interaction: A comparison of different discretization and solution approaches." Fluid Structure Interaction II. Springer, Berlin, Heidelberg, 2011. 413-424.
13. Griffith, B. E., and Xiaoyu Luo."Hybrid finite difference/finite element version of the immersed boundary method." International Journal for Numererical Methods in Engineering 1-26 (Submitted in revised form, 2012) DOI: 10.1002/nme.
14. Hesch, C., et al."A mortar approach for fluid-structure interaction problems: Immersed strategies for deformable and rigid bodies." Computer Methods in Applied Mechanics and Engineering 278 (2014): 853-882.